Crystal structure refinement of Co-doped lanthanum chromites

H. P. S. Corrêa and C. O. Paiva-Santos
Instituto de Química, Universidade Estadual Paulista (UNESP), R. Professor Degni s/n, 14800-900 Araraquara, São Paulo, Brazil

L. F. Setz, L. G. Martinez, and S. R. H. Mello-Castanho
Instituto de Pesquisas Energéticas e Nucleares (IPEN), Campus Universidade de São Paulo (USP), 05508-900 São Paulo, São Paulo, Brazil

M. T. D. Orlando
Departamento de Física e Química, Universidade Federal do Espírito Santo (UFES), Vitória, Espírito Santo, Brazil

(Received 16 May 2007; accepted 28 February 2008)

Results of crystal structure refinements and phase quantification for samples of Co-doped lanthanum chromites with nominal composition $LaCr_{1-x}Co_xO_3$, for $x=0.00$, 0.10, 0.20, and 0.30, prepared by combustion synthesis are presented. The resulting powders were characterized by scanning electron microscopy and X-ray diffraction (XRD). The XRD patterns were obtained with Cu $K\alpha$ radiation for non-doped lanthanum chromite sample and additionally with Cr $K\alpha$ radiation for Co-doped lanthanum chromites samples, in order to enhance the signal from scattering. Rietveld analysis of XRD data showed that the studied samples presented the lanthanum chromite with an orthorhombic structure (*Pnma*), except for the composition with $x=0.30$, in which the space group was found to be $R\bar{3}c$. © *2008 International Centre for Diffraction Data.* [DOI: 10.1154/1.2903501]

Key words: $LaCrO_3$, lanthanum chromite, Rietveld, X-ray diffraction

I. INTRODUCTION

Doped lanthanum chromites are used in high-temperature solid oxide fuel cells as interconnect material, because of their refractory nature, corrosion resistance (stability during the fuel cell operation), and the possibility of doping to improve (*p*-type) electronic conductivity (Minh, 1993; Badwal 2001; Fergus, 2004; Hrovat *et al.*, 1995). Naray-Szabo (1943) and Wold and Ward (1954) are the first to report on the crystalline structure of lanthanum chromite ($LaCrO_3$). The authors propose a perovskite-type cubic structure, space group $Pm\bar{3}m$, with lattice parameter of approximately 3.90 Å. By means of neutron diffraction, Khattak and Cox (1977) observed that at room temperature, $LaCrO_3$ has an orthorhombic structure, space group *Pnma*, with lattice parameters 5.475, 7.754, and 5.513 Å (see Figure 1). Several other authors refer to $LaCrO_3$ as a compound presenting a distorted perovskite-type structure at room temperature (Taguchi *et al.*, 1995; Taguchi *et al.*, 1999; Sakai *et al.*, 1996; Oikawa *et al.*, 2000; Hashimoto *et al.*, 2000).

Substitutions at *A* sites, *B* sites, or both, can result in strongly enhanced electrical properties and compatibility with other cell components, concerning thermal expansion properties. This is the case of Ca-doped, Sr-doped, Mg-doped (Mori *et al.*, 1997), and Ni-doped (Berger *et al.*, 2001) $LaCrO_3$, for instance. These doping atoms are also used to reduce densification times, densification temperatures, or both, because of its high stability (Simner *et al.*, 1999). The doping of $LaCrO_3$ with a lower-valence ion influences not only the properties of the material, in many ways, but also the phase transformation. For instance, the orthorhombic-rhombohedral transformation of doped $LaCrO_3$ depends on the specific doping atoms. Strontium substitution lowers the transformation temperature, stabilizing the rhombohedral structure at room temperature (Mori *et al.*, 1997), but nickel and calcium substitution raises the transformation temperature (Tolochko *et al.*, 1987). Magnesium substitution, on the other hand, does not affect the orthorhombic-rhombohedral transformation temperature (Srilomsak *et al.*, 1989). The purpose of this work is to report the influence of the Co-doping in stabilizing the rhombohedral structure at room temperature. The Co-doped $LaCrO_3$ powders studied in this work were synthesized using the combustion synthesis technique in air (Setz *et al.*, 2006).

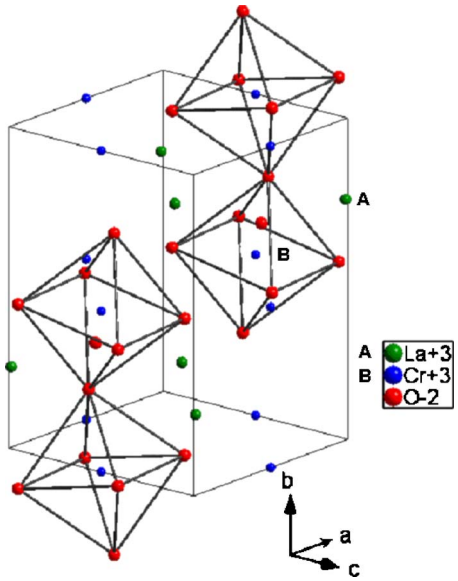

Figure 1. (Color online) Structure of orthorhombic $LaCrO_3$ (space group *Pnma*, distorted perovskite-type).

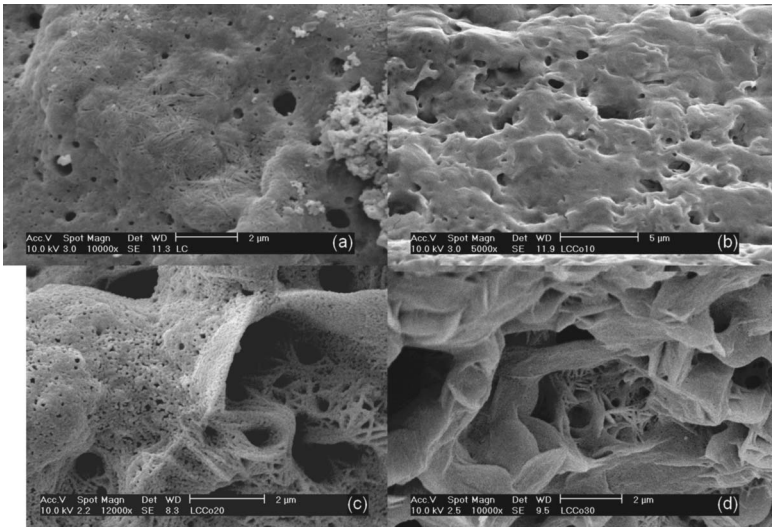

Figure 2. Scanning electron microscopy of samples (a) LC, (b) LCCo10, (c) LCCo20, and (d) LCCo30.

II. EXPERIMENTAL

A. Samples

Among the many synthesis techniques for $LaCrO_3$, combustion synthesis was chosen because it consists of a relatively simple and fast method (Setz *et al.*, 2006). For the synthesis of Co-doped $LaCrO_3$, the following reagents were used: chromium(III) nitrate(III) nonahydrate P.A. $[Cr(NO_3)_3 \cdot 9H_2O]$ (99%, Aldrich, Saint Louis, Missouri), lanthanum(III) nitrate hexahydrate P.A. $(La(NO_3)_3 \cdot 6H_2O)$ (99.99%, Aldrich, Saint Louis, Missouri), cobalt(II) nitrate hexahydrate P.A. $[Co(NO_3)_2 \cdot 6H_2O]$ (98%, Vetec Química, Rio de Janeiro, Brazil), and Urea P.A. $[(NH_2)_2CO]$ (Nuclear, São Paulo, Brazil). The solutions were prepared according to stoichiometric compositions $LaCr_{1-x}Co_xO_3$, for $x=0.00$, 0.10, 0.20, and 0.30. For the synthesis, the nitrates were stoichiometrically mixed in water and urea. Next, the mixture was slowly warmed up and evaporation of water occurred until the beginning of the reaction, which occurred quickly, with vapor release. The synthesis was carried through in a hot blanket. The molar ratio of urea to lanthanum nitrate used in all compositions was 4:1, and the studied compositions with their respective symbols are presented in Table I.

B. Scanning electron microscopy, X-ray diffraction, and refinement

Morphological analysis by SEM was performed on the resulting powders at the condition they were obtained using a Philips XL30 electron microscopy. Part of the powders were also ground in an agate mortar and sieved in a #325 mesh (45 μm aperture) and then characterized by XRD. XRD measurements were performed using a Rigaku DMAX diffractometer with Cu $K\alpha$ radiation (1.5406 Å) for sample $LaCrO_3$ (LC) and also Cr $K\alpha$ radiation (2.2897 Å) for $LaCr_{1-x}Co_xO_3$ (Co-doped) samples. Anomalous X-ray scattering was used in order to enhance the contrast between Cr and Co atoms. The diffraction data were obtained from 20 to $120° 2\theta$ at 0.02° steps for sample LC and from 30 to $130° 2\theta$ at 0.02° steps for Co-doped samples, using $\frac{1}{2}°$ divergence slit, 0.3 mm receiving slit, 40 kV, and 30 mA. The instrumental broadening was obtained from fitting to data of standard Al_2O_3 sample [NIST standard reference material 676 (NIST, 2005)].

The Rietveld refinements were performed using the program GSAS (Larson and Von Dreele, 2000) with the interface EXPGUI (Toby, 2001). The peak profile function was modeled using a convolution of the Thompson-Cox-Hastings pseudo-Voigt function (Thompson *et al.*, 1987) with the asymmetry correction described by Finger *et al.* (1994) to account for the asymmetry attributable to axial divergence. In order to account for the anisotropy in the half-width of the reflections, the bi-dimensional model described by Larson and Von Dreele (2000) was used for crystallite size and the model described by Stephens (1999) was used for anisotropic strain. The background was fitted by shifted Chebyschev function (Larson and Von Dreele, 2000) with eight terms. The initial crystal structure data for the refinements of $LaCrO_3$ were the models reported by Tezuka *et al.* (1998) for the rhombohedral phase and by Taguchi *et al.* (1999) for the orthorhombic and rhombohedral phases. Constraints were applied to the cations Co^{3+} and Cr^{3+} during the refinements in order for the position and isotropic atom displacement parameters to stay the same. For the refinement of the occupation factor, a constraint was applied to keep the sum of the occupancies equal to 1.0. The oxygen anions were constrained to all have the same isotropic atomic displacement parameter.

TABLE I. Studied compositions and respective symbols.

Symbol	Nominal composition
LC	$LaCrO_3$
LCCo10	$LaCr_{0.90}Co_{0.10}O_3$
LCCo20	$LaCr_{0.80}Co_{0.20}O_3$
LCCo30	$LaCr_{0.70}Co_{0.30}O_3$
LC	$LaCrO_3$

III. RESULTS AND DISCUSSION

A. Scanning electron microscopy

Figure 2 shows scanning electron micrographs of the samples. The powders present an aspect of porous flocks;

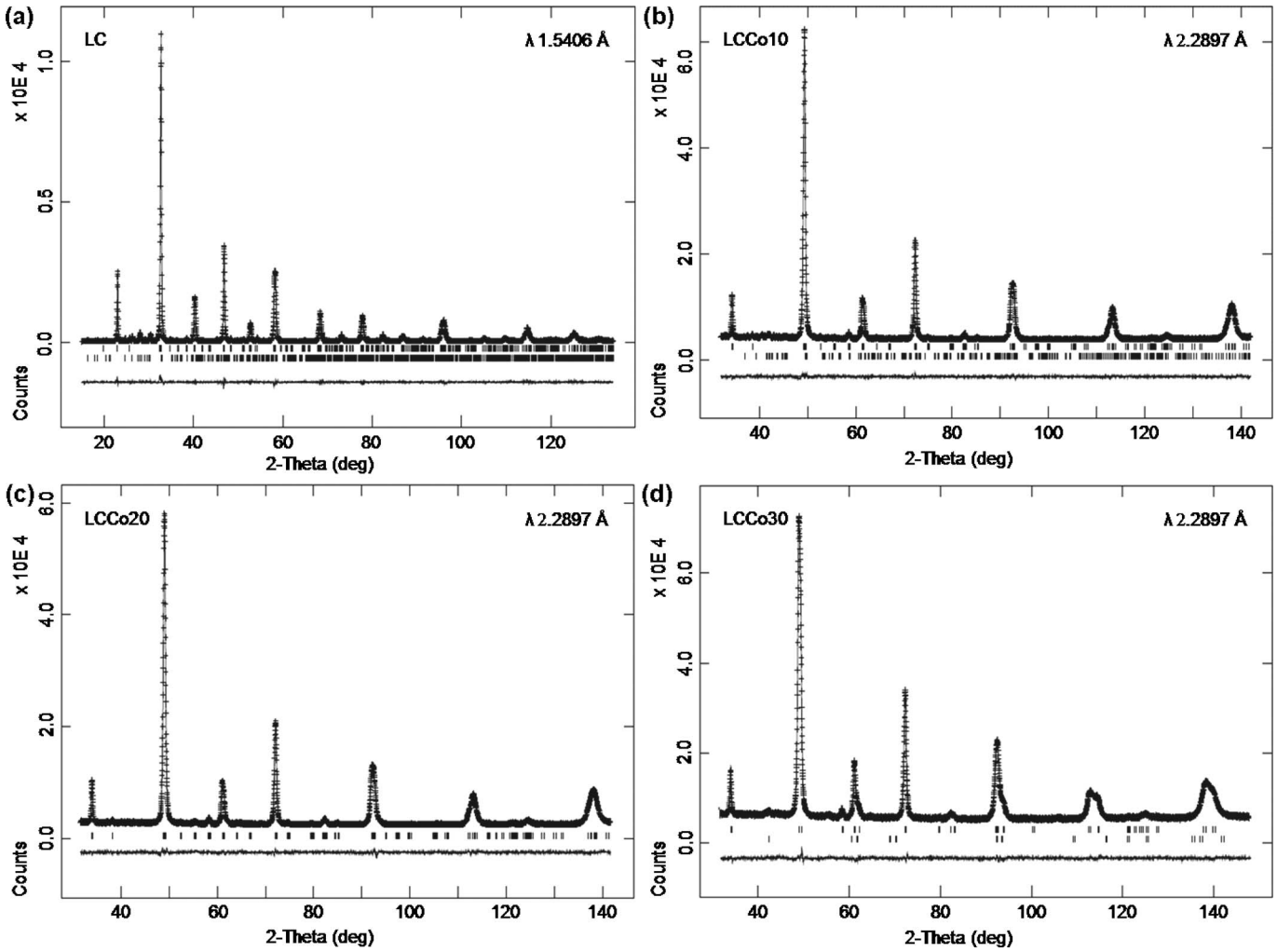

Figure 3. X-ray diffraction pattern for the samples with the Rietveld-fitted pattern and the difference plot: (a) LC, (b) LCCo10, (c) LCCo20, and (d) LCCo30.

i.e., surfaces with the appearance of sponges. As a general remark, the observed shape was similar for all studied samples, namely, sponges constituted by extremely fine particles of submicrometric (or nanometric) dimensions, with irregular shapes and fragile aspects, meaning easy desegregation, with several holes attributable to significant gas release during the combustion reaction. With the increase in the concentration of cobalt, for the samples of the series $LaCr_{1-x}Co_xO_3$, the tendency for preferred orientation in the formation of the sponge can be observed, as demonstrated in Figures 2(c) and 2(d) for samples LCCo20 ($x=0.2$) and LCCo30 ($x=0.3$), respectively. This can be associated to the presence of cobalt nitrate in the combustion reaction, which in larger quantities, causes the release of larger amounts of heat, observed during the sample preparation procedures.

B. X-ray diffraction and refinement

X-ray patterns recorded for non-doped (LC) and doped ($LaCr_{1-x}Co_xO_3$) lanthanum chromite samples are shown in Figure 3. The XRD pattern for the LC sample shows two phases: a $LaCrO_3$ phase crystallized in an orthorhombic symmetry [*Pnma*—PDF 33-701 (ICDD, 2005)] and a small amount of $LaCrO_4$ [$P2_1/n$—PDF 49-1710 (ICDD, 2005)]. For the samples of $LaCr_{1-x}Co_xO_3$ series, except for LCCo30, XRD patterns show reflections corresponding to orthorhombic lanthanum chromite. It is an indication that their crystal structures are similar to that in the LC sample, i.e., *Pnma* symmetry, with slight differences in lattice parameters. In LCCo30 the doped $LaCrO_3$ crystallized in a different structure, namely, rhombohedral symmetry [$R\bar{3}c$—PDF 33-702 (ICDD, 2005)], indicating that this phase is stable at room temperature with 30% cobalt substitution. Small amounts of $LaCrO_4$ and CrO_2 [$P4_2/mnm$—PDF 84-1818 (ICDD, 2005)] phases were observed in LCCo10 and LCCo30 samples, respectively.

Table II presents the results for phase quantification for LC and $LaCr_{1-x}Co_xO_3$ series samples. The quantity of lanthanum chromite phase (*Pnma*) is greater than 90% for all samples and reached 100% for the LCCo20 sample. Table III presents the refined crystal structure parameters and reliability factors of the Rietveld analysis; plots of diffraction data and their Rietveld fits are given in Figures 3(a)–3(d) for the non-doped and doped $LaCrO_3$. With the substitution of Cr by Co atom on the *B* site of the perovskite structure, a decrease of lattice parameters *a*, *b*, and *c*, and, consequently, a reduction in the unit cell volume is observed.

Figure 4 shows a linear dependence between the volume cell (divided by *Z*) and the dopant concentration, for the

TABLE II. Results for phase quantification for LC and $LaCr_{1-x}Co_xO_3$ series samples.

Sample	Phases	wt%
LC	Non-doped LaCrO3	92.15(8)
	LaCrO4	7.85(12)
LCCo10	Doped LaCrO3	91.99(9)
	LaCrO4	8.01(11)
LCCo20	Doped LaCrO3	100
LCCo30	Doped LaCrO3	91.67(9)
	CrO2	8.33(10)

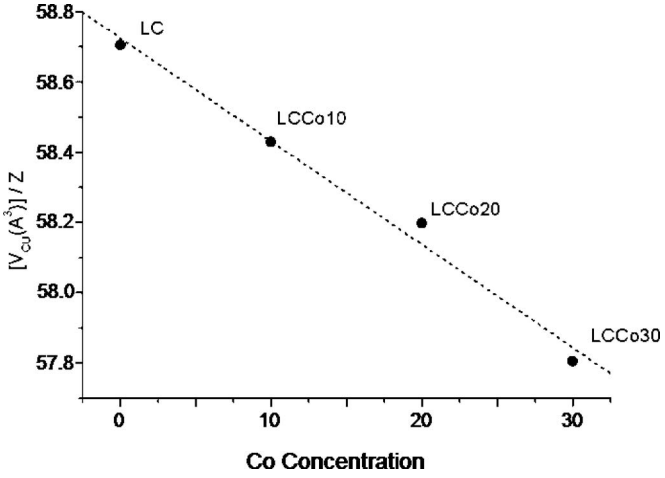

Figure 4. V/Z (cell volume/number of formula units) in the unit cell × Co concentration.

$LaCr_{1-x}Co_xO_3$ series, obeying Vegard's law (Dentun and Ashcroft, 1991). The volume shrinks by 1.5% as a result of Co substitution, for the doping range studied. This behavior is explained by the exchange of the Cr^{3+} ion (radius 0.615 Å) with the Co^{3+} ion (smaller radius 0.545 Å) at the *B* site of the perovskite structure [values for radii obtained from Shannon (1976)]. This difference between the ionic radii can also explain the orthorhombic and rhombohedral structures found. It is well known that the crystal structures of ABO_3 perovskites are related to the Goldschmidt tolerance factor defined as $t=(R_A+R_O)/2^{1/2}(R_B+R_O)$, R_A, R_B, and R_O being the ionic radii for *A*, *B*, and oxygen atoms, respectively. In general, a purely cubic structure presents $t=1$, but for $LaCrO_3$ and $LaCoO_3$, t is equal to 0.903 and 0.937, respectively, which indicates that they should have crystal structures slightly distorted from the cubic one, as observed. Values of t slightly less than 1 lead to rhombohedral unit cells, and orthorhombic cells are observed for t significantly smaller than 1. From this experiment, the rhombohedral to orthorhombic phase transition t value at room temperature seems to be located at $x\sim0.3$ for this series.

IV. CONCLUSION

Combustion reaction is a suitable method for the production of cobalt-doped lanthanum chromite. Powder X-ray diffraction, followed by Rietveld analysis, was essential in obtaining structural information of the materials including lattice parameters, composition, and mainly the quantitative

TABLE III. Refined crystal structure parameters and the reliability factors in Rietveld analysis for the non-doped and doped $LaCrO_3$.

Sample—phase, space group	Site	Occ.	*x*	*y*	*z*	U_{iso} (Å)	*Z* (Å^3)	Composition	R_w(%), R_F^2(%), χ^2
LC—non-doped	La^{3+} 4(*c*)		0.01818(10)	1/4	0.00412(23)	0.0066(1)	234.81	$LaCrO_3$	8.37, 2.96, 1.281
Orthorhombic	Cr^{3+} 4(*b*)		0	0	1/2	0.0039(2)	4		
Pnma	O^{2-} 4(*c*)		0.4904(12)	1/4	−0.0616(15)	0.0121(4)			
	O^{2-} 8(*d*)		−0.2729(15)	0.5354(8)	0.7291(15)	0.0122(11)			
a=5.4800(1), *b*=7.7631(2), *c*=5.5195(1)									
LCCo10—doped	La^{3+} 4(*c*)		0.01704(9)	1/4	0.00282(25)	0.0067(1)	233.67	$LaCr_{0.90}Co_{0.10}O_3$	2.00, 1.98, 1.384
Orthorhombic	Cr^{3+} 4(*b*)	0.9	0	0	1/2	0.0027(2)	4		
Pnma	Co^{3+} 4(*b*)	0.1	0	0	1/2	0.0027(2)			
	O^{2-} 4(*c*)		0.4983(8)	1/4	−0.0647(8)	0.0111(2)			
	O^{2-} 8(*d*)		−0.2768(9)	0.5327(4)	0.7245(8)	0.0086(6)			
a=5.4709(1), *b*=7.7510(1), *c*=5.5115(1)									
LCCo20—doped	La^{3+} 4(*c*)		0.01530(11)	1/4	0.00320(26)	0.0064(1)	232.51	$LaCr_{0.80}Co_{0.20}O_3$	2.12, 1.50, 1.447
Orthorhombic	Cr^{3+} 4(*b*)	0.8	0	0	1/2	0.0043(2)	4		
Pnma	Co^{3+} 4(*b*)	0.2	0	0	1/2	0.0043(2)			
	O^{2-} 4(*c*)		0.4951(10)	1/4	−0.0662(8)	0.0113(2)			
	O^{2-} 8(*d*)		−0.2829(9)	0.5291(5)	0.7202(5)	0.0090(7)			
a=5.4633(1), *b*=7.7402(1), *c*=5.5050(1)									
LCCo30—doped	La^{3+} 6(*a*)		0	0	1/4	0.0065(1)	115.61	$LaCr_{0.70}Co_{0.30}O_3$	2.03, 1.54, 1.370
Rhombohedric	Cr^{3+} 6(*b*)	0.7	0	0	0	0.0037(1)	2		
$R\bar{3}c$	Co^{3+} 6(*b*)	0.3	0	0	0	0.0037(1)			
	O^{2-} 18(*e*)		0.1935(4)	0.3065(4)	1/4	0.0122(1)			
a=5.44377(1), α=115.61(1)°									

analysis of the phases present in the samples. The studied compounds of Co-doped $LaCrO_3$ ($LaCr_{1-x}Co_xO_3$) presented 100% of the desired phase for LCCo20 sample. The LCCo30 sample presented 91.7% of the composition $LaCr_{0.70}Co_{0.30}O_3$ with a rhombohedral crystal structure and space group symmetry $R\bar{3}c$, indicating that this rhombohedral phase is stable at room temperature with 30% cobalt substitution.

ACKNOWLEDGMENT

The authors thank Brazilian national scientific agency CAPES for financial support.

Badwal, S. P. S. (**2001**). "Stability of solid oxide fuel cell components," Solid State Ionics **143**, 39–46.

Berger, D., Jitaru, I., Stanica, N., Perego, R., and Schoonman, J. (**2001**). "Complex precursors for doped lanthanum chromite synthesis," J. Mater. Synth. Process. **9**, 137–142.

Denton, A. R., and Ashcroft, N. W. (**1991**). "Vegard's law," Phys. Rev. A **43**, 3161–3164.

Fergus, J. W. (**2004**). "Lanthanum chromite-based materials for solid oxide fuel cell interconnects," Solid State Ionics **171**, 1–15.

Finger, L. W., Cox, D. E., and Jephcoat, A. P. (**1994**). "A correction for powder diffraction peak asymmetry due to axial divergence," J. Appl. Crystallogr. **27**, 892–900.

Hashimoto, T., Tsuzuki, N., Kishi, A., Takagi, K., Tsuda, K., Tanaka, M., Oikawa, K., Kamiyama, T., Yoshida, K., Tagawa, H., and Dokiya, M. (**2000**). "Analysis of crystal structure and phase transition of $LaCrO_3$ by various diffraction measurements," Solid State Ionics **132**, 181–188.

Hrovat, M., Bernik, S., Holc, J., Kolar, D., and Dacar, B. (**1995**). "Preliminary data on subsolidus phase equilibria in the La_2O_3-Cr_2O_3-Y_2O_3 and La_2O_3-Cr_2O_3-ZrO_2 systems," J. Mater. Sci. Lett. **14**, 1684–1687.

ICDD (**2005**). "Powder Diffraction File," *International Centre for Diffraction Data*, edited by W. F. McClune, Newtown Square, PA, 19073-3272.

Khattak, C. P., and Cox, D. E. (**1977**). "Profile analysis of X-ray powder diffractometer data: structural refinement of $La_{0.75}Sr_{0.25}CrO_3$," J. Appl. Crystallogr. **10**, 405–411.

Larson, A. C., and Von Dreele, R. B. (**2000**). *General Structure Analysis System (GSAS)* (Report LAUR 86–748) (Los Alamos National Laboratory, Los Alamos, New Mexico).

Minh, N. Q. (**1993**). "Ceramic fuel cells," J. Am. Ceram. Soc. **76**, 563–588.

Mori, M., Yamamoto, T., Itoh, H., and Watanabe, T. (**1997**). "Compatibility of alkaline earth metal (Mg, Ca, Sr)-doped lanthanum chromites as separators in planar-type high-temperature solid oxide fuel cells," J. Mater. Sci. **32**, 2423–2431.

Naray-Szabo, S. (**1943**). "Die Strukturen von Verbindungen ABO_3 Schwester Strukturen," Naturwiss. **31**, 466–467.

NIST (**2005**). *Certificate of Analysis, Standard Reference Material 676, Alumina Internal Standard* (National Institute of Standards and Technology, Gaithersburg, Maryland) ⟨https://srmors.nist.gov/view_cert.cfm?srm=676⟩.

Oikawa, K., Kamiyama, T., Hashimoto, T., Shimojyo, Y., and Morii, Y. (**2000**). "Structural phase transition of orthorhombic $LaCrO_3$ studied by neutron powder diffraction," J. Solid State Chem. **154**, 524–529.

Sakai, N., Fjellvâg, H., and Hauback, B. C. (**1996**). "Structural, magnetic, and thermal properties of $La_{1-t}Ca_tCrO_{3-\delta}$," J. Solid State Chem. **121**, 202–213.

Setz, L. F. G., Corrêa, H. P. S., Paiva-Santos, C. O., and Mello-Castanho, S. R. H. (**2006**). "Sintering of cobalt and strontium doped lanthanum chromite obtained by combustion synthesis," Mater. Sci. Forum **530–531**, 671–676.

Shannon, R. D. (**1976**). "Revised effective ionic radii and systematic studies of interatomic distances in halides and chalcogenides," Acta Crystallogr., Sect. A: Cryst. Phys., Diffr., Theor. Gen. Crystallogr. **32**, 751–767.

Simner, S., Hardy, J., Stevenson, J., and Armstrong, T. (**1999**). "Sintering mechanisms in strontium doped lanthanum chromite," J. Mater. Sci. **34**, 5721–5732.

Srilomsak, S., Schilling, D., and Anderson, H. (**1989**). "Expansion studies on cathode and interconnect oxides," in *First International Symposium on Solid Oxide Fuel Cells*, edited by S. C. Singhal (Electrochemical Society, Pennington, New Jersey), Vol. 89–11, pp. 129–140.

Stephens, P. W. (**1999**). "Phenomenological model of anisotropic peak broadening in powder diffraction," J. Appl. Crystallogr. **32**, 281–289.

Taguchi, H., Matsu-ura, S., Nagao, M. and Kido, H. (**1999**). "Electrical properties of perovskite-type $La(Cr_{1-x}Mn_x)O_{3+\delta}$," Physica B **270**, 325–331.

Taguchi, H., Nagao, M., and Takeda, Y. (**1995**). "Relationship between the electrical properties and crystal structure of $(La_{1-x}Nd_x)CrO_3$ ($0 \leqslant x \leqslant 1.0$)," J. Solid State Chem. **114**, 236–241.

Tezuka, K., Hinatsu, Y., Nakamura, A., Inami, T., Shimojo, Y., and Morii, Y. (**1998**). "Magnetic and neutron diffraction study on perovskites $La_{1-x}Sr_xCrO_3$," J. Solid State Chem. **141**, 404–410.

Thompson, P., Cox, D. E., and Hastings, J. B. (**1987**). "Rietveld refinement of Debye-Scherrer synchrotron X-ray data from Al_2O_3," J. Appl. Crystallogr. **20**, 79–83.

Toby, B. H. (**2001**). "*EXPGUI*, a graphical user interface for *GSAS*," J. Appl. Crystallogr. **34**, 210–213.

Tolochko, S. P., Kononyuk, I. F., Lyutsko, V. A., and Zonov, Y. G. (**1987**). "Phase transitions in solid solutions based on lanthanum chromite," Inorg. Mater. **23**, 1342–1345.

Wold, A., and Ward, R. (**1954**). "Perovskite-type oxides of cobalt, chromium and vanadium with some rare earth elements," J. Am. Chem. Soc. **76**, 1029–1030.